Proceedings of the 12th International Conference on Quasicrystals (ICQ12)

Tiling Vertices and the Spacing Distribution of Their Radial Projection

T. Jakobi*

Fakultät für Mathematik, Universität Bielefeld, Universitätsstr. 25, D-33615 Bielefeld, Germany

The Fourier-based diffraction approach is an established method to extract order and symmetry properties from a given point set. We want to investigate a different method for planar sets which works in direct space and relies on reduction of the point set information to its angular component relative to a chosen reference frame. The object of interest is the distribution of the spacings of these angular components, which can for instance be encoded as a density function on $\mathbb{R}_+$. In fact, this radial projection method is not entirely new, and the most natural choice of a point set, the integer lattice $\mathbb{Z}^2$, is already well understood. We focus on the radial projection of aperiodic point sets and study the relation between the resulting distribution and properties of the underlying tiling, like symmetry, order and the algebraic type of the inflation multiplier.

DOI: 10.12693/APhysPolA.126.493

PACS: 45.30.+s, 61.44.Br

1. Radial projection method

Given a locally finite point set $\varLambda \subset \mathbb{R}^2$, the following procedure is applied (see Fig. 1 for an example):

(a) For a reference point $x_0 \in \varLambda$ determine the subset $\varLambda'$ of points visible from this x_0. We call a point p invisible if there exists a $p_0 \in \varLambda$ such that

$$\exists\, t \in (0,1) : p_0 = x_0 + t(p - x_0). \tag{1}$$

(b) Select a radius $R > 0$ and project all $x \in \varLambda' \cap B_{\mathrm{R}}(x_0)$ to $\partial B_{\mathrm{R}}(x_0)$. If x is given as $(a,b) \in \mathbb{R}^2$, then this amounts to mapping x to $\arctan(b/a)$.

(c) The step in (b) produces a list of distinct (because of the visibility condition) angles $\varPhi(R)$. Since $\varLambda$ is locally finite, we can sort the list

$$\varPhi(R) = \{\varphi_1, \ldots, \varphi_n\}$$

in ascending order. We also renormalise the φ_i with the factor $\frac{n}{2\pi}$, such that the mean distance between consecutive entries becomes 1.

(d) Define $d_i := \varphi_{i+1} - \varphi_i$ and consider the discrete probability measure

$$\nu_{\mathrm{R}} := \frac{1}{n-1} \sum_{i=1}^{n-1} \delta_{d_i}.$$

(e) Assuming that it exists, the spacing distribution is now obtained by taking the limit $R \to \infty$ in the sense of weak convergence of measures.

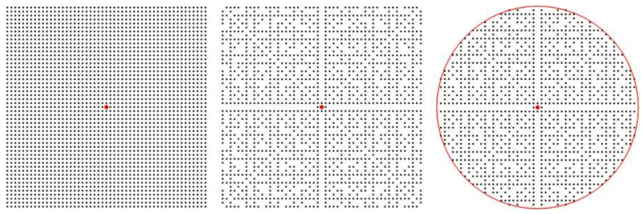

Fig. 1. Radial projection using the example of the $\mathbb{Z}^2$ lattice.

The choice of the point x_0 can be arbitrary and, in general the limit measure $\nu := \lim_{R\to\infty} \nu_{\mathrm{R}}$ depends on it. For now, we restrict ourselves to reference points with *high symmetry* (see Sect. 4, Figs. 2 and 3). Further investigations are needed to decide whether an averaging over multiple x_0 makes more sense here.

All results (except for the reference cases) are currently strictly numerical and therefore rely on the computation of large circular patches of the point set and the determination of visibility. For an introduction to the topic of aperiodic tilings we refer to [1].

2. Integer lattice $\mathbb{Z}^2$

The lattice $\mathbb{Z}^2$ provides the most ordered case of a planar point set. In this regard, it represents one reference point set for a potential classification of order. The set of visible points from the origin is given by

$$V_{\mathbb{Z}^2} = \{(a,b) \in \mathbb{Z}^2 : \gcd(a,b) = 1\}. \tag{2}$$

In 2000, a closed expression [2] was derived for the limiting measure. With our setup, the explicit density function reads

$$g(t) = \begin{cases} 0, & 0 < t < \frac{3}{\pi^2}, \\ \frac{6}{\pi^2 t^2} \log \frac{\pi^2 t}{3}, & \frac{3}{\pi^2} < t < \frac{12}{\pi^2}, \\ \frac{12}{\pi^2 t^2} \log\left(2 \Big/ \left(1 + \sqrt{1 - \frac{12}{\pi^2 t}}\right)\right), & \frac{12}{\pi^2} < t, \end{cases}$$

but in fact the existence also holds for more general expanding regions (which is a circle here). A Taylor expansion of the tail of $g(t)$ gives

*e-mail: tjakobi@math.uni-bielefeld.de

$$g(1/t) = \frac{36}{\pi^4}t^3 + \frac{162}{\pi^6}t^4 + \mathcal{O}(t^5) \quad \text{for } t \to 0_+, \qquad (3)$$

making it obvious that the moments of order $k \geq 2$ do not exist. A plot of $g(t)$ is overlayed over most histograms (see e.g. Sect. 4, Figs. 5 and 6). For all other cases (apart from the next), only histograms were computed.

3. Poisson distributed points

In contrast to the $\mathbb{Z}^2$ case, the point set generated by a homogeneous spatial Poisson process gives us the other reference point for our classification. In terms of order, it represents the case of total disorder. The model is also known as *complete spatial randomness* (CSR) or *ideal gas* in terms of physics.

Application of the radial projection procedure, with an arbitrary choice of reference point, yields a 1-dimensional CSR with intensity $\lambda = 1$ (due to the normalisation) in step (c). From there, it is not hard to see that the density of the radial projection measure is given by

$$f_\lambda(x) = \begin{cases} \lambda \exp(-\lambda x), & x \geq 0, \\ 0, & x < 0, \end{cases}$$

since step (d) just asks the question what the distribution of the waiting time between jumps of the process is.

The density $f_\lambda(x)$ (a plot can be seen in Fig. 9) therefore provides the second explicit function that we can test histograms against.

4. Cyclotomic model sets and visibility

Many aperiodic tilings cannot only be realised by inflation of a set of prototiles, but by projecting a higher-dimensional lattice into $\mathbb{R}^2$. This is often described as the *cut and project* method or *model set* description.

Our general interest is in *cyclotomic* model sets, since these can be used to construct n-fold symmetric tilings. Also, this description is more suitable for radial projection since it only gives the tiling vertices and allows precise control over the patch size.

The Ammann–Beenker (AB) and the Tübingen triangle (TT) tiling can both be described as a cyclotomic model set (CMS) and the tiling vertices (the tiling in Fig. 2 uses the triangle/rhombus version) are given by

$$T_{\mathsf{AB}} = \{x \in \mathbb{Z}[\zeta_8] : x^\star \in W_8\},$$
$$T_{\mathsf{TT}} = \{x \in \mathbb{Z}[\zeta_5] : x^\star \in W_{10} + \epsilon\},$$

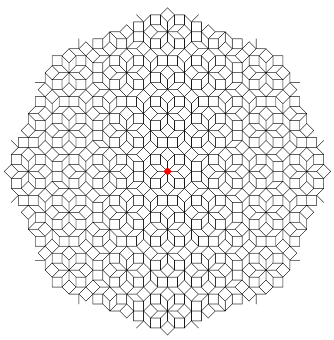

Fig. 2. AB patch generated via projection.

where the window W_8 is a regular octagon with edge length 1 centered at the origin.

For the TT tiling the window W_{10} is a decagon, here with edge length $\sqrt{(\tau+2)/5}$ (τ denoting the golden mean), Fig. 3. For the orientations of the windows, see Fig. 4. The map $\star$ is given by the extension of $\zeta_8 \mapsto \zeta_8^3$ in the AB case, and $\zeta_5 \mapsto \zeta_5^2$ in the TT one ($\zeta_n = \exp(2\pi \mathrm{i}/n)$), Figs. 5 and 6.

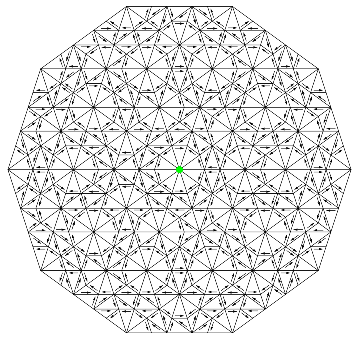

Fig. 3. TT patch generated via inflation.

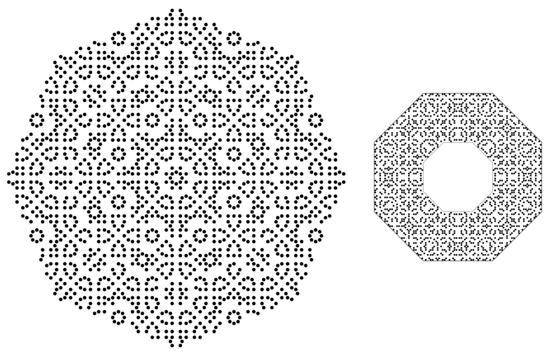

Fig. 4. Visible vertices of the 8-fold AB tiling (left: direct space, right: internal space).

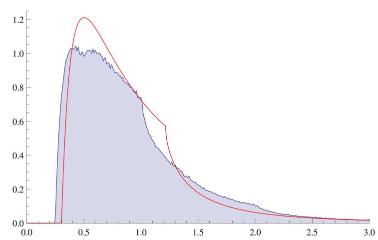

Fig. 5. Spacing distribution of a large AB patch.

Another aspect of choosing this description is that the visibility test in Eq. (1) is computationally expensive compared to the local test (2) of the $\mathbb{Z}^2$ case. It turns out that a CMS also admits a similar description. For example, the visible points of the AB tiling with the reference point at the origin are

$$V_{\mathsf{AB}} = \{x \in T_{\mathsf{AB}} : \lambda_{\mathrm{sm}} x^\star \notin W_8 \text{ and } x \text{ is coprime}\},$$

with $\lambda_{\mathrm{sm}} = 1 + \sqrt{2}$, the silver mean. The $\mathbb{Z}$-module in

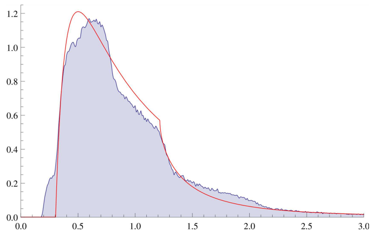

Fig. 6. Spacing distribution of a large TT patch.

this case can be decomposed into $\mathbb{Z}[\zeta_8] = \mathbb{Z}[\sqrt{2}] \oplus \mathbb{Z}[\sqrt{2}]\zeta_8$ and coprime in this context means that for $\mathbb{Z}[\zeta_8] \ni x = x_1 + x_2\zeta_8$ the $\gcd(x_1, x_2)$ is a unit in $\mathbb{Z}[\sqrt{2}]$.

The same description can be given for the TT tiling and reads

$$V_{\mathsf{TT}} = \{x \in T_{\mathsf{TT}} : \tau x^\star \notin W_{10} + \epsilon \text{ and } x \text{ is coprime}\},$$

with ϵ a small shift. Coprimality is defined as in the AB case, except that the module is $\mathbb{Z}[\tau]$ this time. The simplicity of these local visibility tests also depends on the order of the underlying cyclotomic field, here a prime power.

5. A 12-fold cyclotomic case

Another tiling that is given by a CMS is the *Gähler shield* (GS) tiling. The vertices are

$$T_{\mathsf{GS}} = \{x \in \mathbb{Z}[\zeta_{12}] : x^\star \in W_{12} + \epsilon\},$$

with a dodecagon W_{12} (edge length 1) and the map $\star$ given by the extension of $\zeta_{12} \mapsto \zeta_{12}^5$. The order of the cyclotomic field leads to a slightly more involved local visibility test

$$V_{\mathsf{GS}} = \{x \in T_{\mathsf{GS}} : n(x) = 1 \wedge \lambda_1 x^\star \notin W_{12} + \epsilon\}$$
$$\cup \{x \in T_{\mathsf{GS}} : n(x) = 2 \wedge \lambda_2 x^\star \notin W_{12} - \epsilon\}.$$

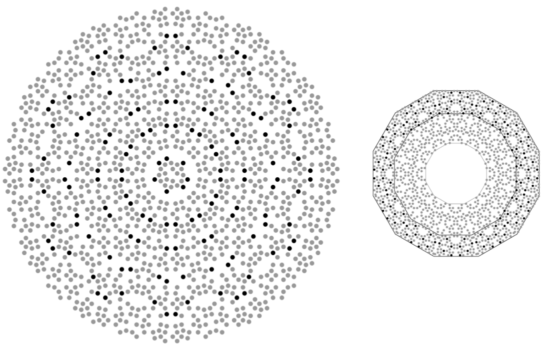

Fig. 7. Visible points of a 12-fold GS tiling (left: direct space, right: internal space).

The function n decomposes a $x \in \mathbb{Z}[\zeta_{12}]$ into the direct-sum representation

$$\mathbb{Z}[\sqrt{3}] \oplus \mathbb{Z}[\sqrt{3}]\zeta_{12} \text{ with } \lambda_{12} := 2 + \sqrt{3}$$

and then computes $|N(\gcd(x_1, x_2))|$, the absolute value of the algebraic norm of the gcd of the components. The two *rescaling factors* for the visibility test are given by

$$\lambda_1 := \sqrt{\lambda_{12}2} \text{ and } \lambda_2 := \sqrt{\lambda_{12}/2}.$$

The first part of the set V_{GS} (indicated in grey in Fig. 7) comprises the already known coprime elements.

The second part is exceptional, and its existence is linked to the order 12 being a composite number.

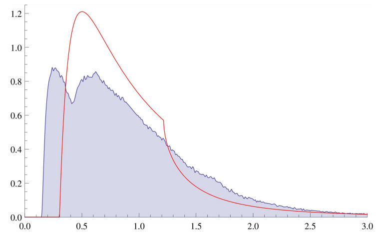

Fig. 8. Spacing distribution of a large GS patch.

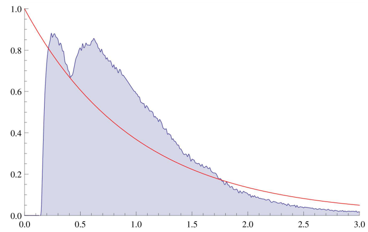

Fig. 9. GS spacing distribution compared against Poisson.

Even though Fig. 8 deviates a lot more from the $\mathbb{Z}^2$ distribution (compared to Figs. 4 and 5), all considered cyclotomic cases exhibit the special threefold structure (gap, bulk, and tail). Let us consider a different tiling with stronger spatial fluctuations, see Fig. 9.

6. A non-Pisot case/Lançon–Billard

The Lançon–Billard (LB) tiling, Fig. 10, is an example of a *chiral* (the tiles only appear in one chirality) inflation tiling with a multiplier $\lambda_{\mathsf{LB}} = \sqrt{(5+\sqrt{5})/2}$, which is a non-Pisot number. The inflation rules (a *stone* inflation is only possible with a fractal tile boundary) generate a very irregular tiling, (Fig. 11).

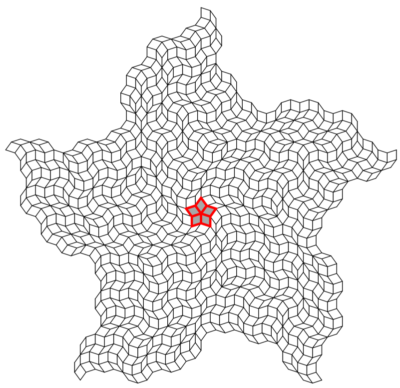

Fig. 10. LB 5-fold symmetric patch.

The resulting distribution shows that the radial projection is sensitive to this irregularity, (Fig. 12).

In fact, on this level, the LB tiling is almost indistinguishable from the Poisson case.

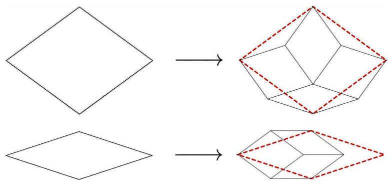

Fig. 11. (top) Tile A maps to $3 \times$ A and $1 \times$ B. (bottom)Tile B maps to $1 \times$ A and $2 \times$ B.

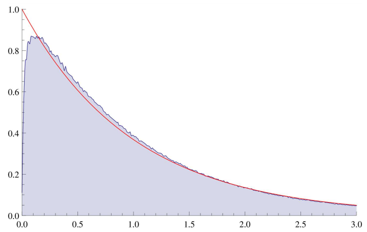

Fig. 12. Spacing distribution of a large LB patch.

7. Some additional examples

We have already seen in Sects. 4 and 5 that the radial projection reacts to the order of symmetry of the tiling. The vertices of the *chair* tiling in Fig. 13 are a subset of $\mathbb{Z}^2$, but a different type of visibility condition has to be applied. The bulk section notices these changes, and shows a lot of structure in general, (Fig. 14).

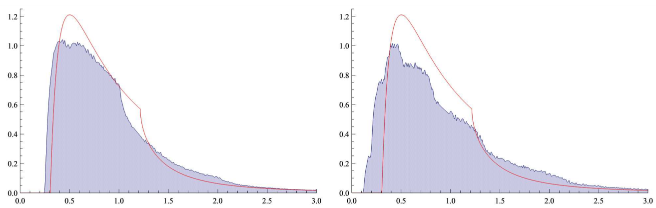

Fig. 13. Spacing distribution of the *chair* (left) and *rhombic Penrose* (right) tiling.

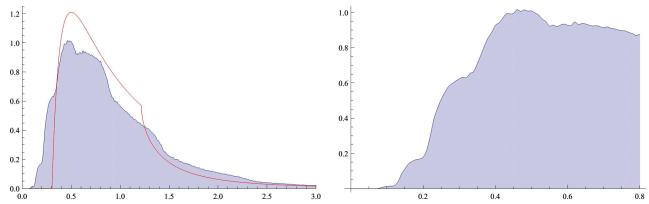

Fig. 14. Spacing distribution of the *Penrose–Robinson* tiling and zoom into the bulk.

8. Tail decay behaviour

The expansion in Eq. (3) gives us an idea how the tail decay of the distribution behaves. A power law fit (c_k the coefficient of t^k) applied to the numerical data indicates that at least the CMS cases also show a similar kind of decay.

Statistical data generated from the radial projection ($e = \text{error} \times 10^{-10}$).

Tiling	Gap size	c_3	c_4	e
$\mathbb{Z}^2$	0.304	0.369	0.168	–
AB	0.222	0.248	0.496	2.79
TT	0.182	0.239	0.513	2.60
GS	0.152	0.232	0.547	4.75

Acknowledgments

The author wishes to thank Michael Baake, Markus Moll and Christian Huck for helpful discussions. This work is supported by the German Research Foundation (DFG) via the Collaborative Research Centre (CRC 701) at the Faculty of Mathematics, University of Bielefeld.

References

[1] M. Baake, U. Grimm, *Aperiodic Order.* Vol. I, *A Mathematical Invitation*, Cambridge University Press, Cambridge 2013.

[2] F.P. Boca, C. Cobeli, A. Zaharescu, *Commun. Math. Phys.* **213**, 433 (2000).